IGNITION AND HEAT RADIATION OF CRYOGENIC HYDROGEN JETS

Friedrich, A.*[1], Breitung, W.[2], Stern, G.[1], Veser, A.[1], Kuznetsov, M.[2], Fast, G.[2], Oechsler, B.[2], Kotchourko, N.[1], Jordan, T.[2], Travis, J.R.[2], Xiao, J.[2], Schwall, M.[2], Rottenecker, M.[2]

[1]Pro-Science GmbH, Parkstrasse 9, Ettlingen, 76275, Germany, surname@pro-science.de
[2]Karlsruhe Institute of Technology, IKET, 76131 Karlsruhe, Germany, surname@kit.edu

ABSTRACT

In the present work release and ignition experiments with horizontal cryogenic hydrogen jets at temperatures of 35 to 65 K and pressures from 0.7 to 3.5 MPa were performed in the ICESAFE facility at KIT. This facility is specially designed for experiments under steady-state sonic release conditions with constant temperature and pressure in the hydrogen reservoir. In distribution experiments the temperature, velocity, turbulence and concentration distribution of hydrogen with different circular nozzle diameters and reservoir conditions was investigated for releases into stagnant ambient air. Subsequent combustion experiments of hydrogen jets included investigations on the stability of the flame and its propagation behavior as function of the ignition position. Furthermore combustion pressures and heat radiation from the sonic jet flame during the combustion process were measured. Safety distances were evaluated and an extrapolation model to other jet conditions was proposed. The results of this work provide novel data on cryogenic sonic hydrogen jets and give information on the hazard potential arising from leaks in liquid hydrogen reservoirs.

1.0 INTRODUCTION

Due to the high density of hydrogen in its liquid phase, transportation and storage of liquid hydrogen at cryogenic temperatures is considered as preferable method in a future hydrogen economy. Further considerations are related to the use of liquid hydrogen as energy carrier and fuel simultaneously, an idea that is developed in the ICEFUEL cable study [1], where pressurized liquid hydrogen (LH2) and superconducting electric power are delivered simultaneously in the same cable to the customer. Information on the hazard potential arising from small leaks in such pipelines carrying liquid hydrogen at high pressures is urgently needed for safety analyses, but only very little information is available so far. In case of a small leak in a prototypical ICEFUEL cable, the blowdown time is much longer than the gas transit time in the free jet, so that the jet structure can adjust practically without delay to the actual pressure and temperature of the hydrogen reservoir in the cable. The jet is in a state of mechanical quasi-equilibrium with its source. The ICESAFE facility was accordingly designed for steady-state release conditions with constant temperature and pressure in the hydrogen reservoir [2].

2.0 EXPERIMENTAL SETUP

2.1 ICESAFE facility

All experiments were performed inside the test chamber of the hydrogen test site HYKA at KIT (Karlsruhe Institute for Technology). With the dimensions 8 x 5.5 x 3.4 m this chamber is much larger than the jet region itself and therefore provides a suitable environment for the experiments on cryogenic free jets. The integrity of the test chamber to the expected loads of the experiments was evaluated in an earlier test series and additionally the chamber is equipped with a powerful and explosion protected ventilation system, so it provided a safe, well defined and reproducible environment for all tests.

The ICESAFE (Integrated Cable Energy Safety Analysis Facility and Equipment) facility was specifically constructed for the investigation of high-pressure discharges of gaseous and liquid hydrogen through small nozzles. It allows investigating stationary sonic hydrogen jets of several meters length into an unobstructed ambience and was designed for a maximum hydrogen flow rate of 10 g/s. For the facility the concept shown in Fig. 1 was realised, which provides high flexibility in the process parameters.

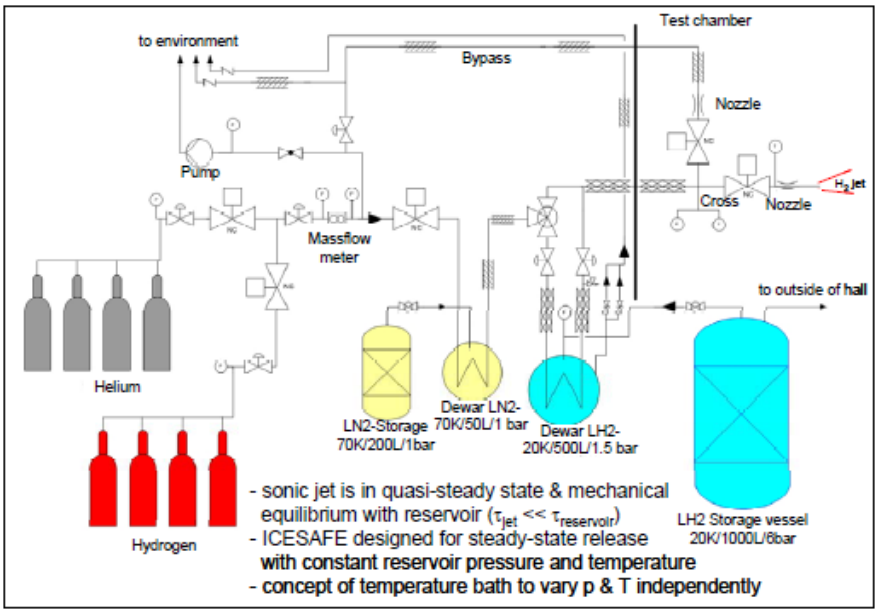

Figure 1: Schematic of the ICESAFE facility.

Gaseous hydrogen from gas cylinders was initially piped through a bath of liquid nitrogen with an exit temperature of about 70 K. Then the pre-cooled hydrogen was conducted into a LH2-dewar where it liquified at a temperature of 20 K, and from where it was then directed towards the release nozzle. The advantage of this design is that the reservoir temperature and pressure can be varied independently and other pressures/temperatures that may be of interest are easily accessible. By switching two remotely operated cryogenic valves (labelled V1 and V2 in Fig. 1) the hydrogen flow can be directed towards the bypass during pre-cooling, or to the release nozzle for the experiment. The powerful ventilation system of the test chamber allows removing the released hydrogen quickly after the completion of a test and re-establishment of known initial conditions of the ambient atmosphere.

2.2 Instrumentation and operation

Pressure gauges, thermocouples (P and T in Fig. 1) and a mass flow meter were used to characterise the hydrogen flow in the ICESAFE facility and its discharge through the nozzle. The pressure and temperature readings at the “cross” were also taken as representative values for the thermodynamic state of the hydrogen in the reservoir, before its discharge through the nozzle. One thermocouple was also installed in the nozzle itself. A gas sampling system, sound level meters, pressure sensors, thermocouples, thermal radiation sensors, background-oriented-schlieren (BOS) photography [3], and high-speed video cameras were applied in the test chamber as additional instrumentation to investigate unignited and ignited hydrogen jets. A LabView program was developed and used to control the hydrogen flow in the ICESAFE facility and to coordinate the data acquisition system inside the test chamber remotely. For the discharge experiments described here, the ICESAFE facility was cooled down to cryogenic hydrogen temperatures (30 K) which took approx. 2.5 hours of cooling time. During the experiments with cold H2 discharge large amounts of GH2, LN2, and LH2 were consumed, and so uninterrupted measurement campaigns were performed until the available LH2 volume (1000 ℓ) was consumed. In the original test procedure the hydrogen was vented through the bypass to the environment until the lowest achievable temperature was recorded at the “cross”. Only then the cold hydrogen was released through the nozzle. In later experiments the cooling gas flow was directed through the nozzle for about 100 s prior to the test to achieve better cooling of valves and nozzle. This cooling hydrogen flow was captured at the nozzle exit with a special ventilation system and not released into the test chamber.

3.0 EXPERIMENTS WITH CRYOGENIC HYDROGEN (34 – 65 K)

Three measurement campaigns with cryogenic hydrogen releases through a small leak were performed in the ICESAFE facility (Table 1). The number of experiments in each of the uninterrupted test series

was limited by the available inventory of liquid hydrogen in the storage tank (1000 ℓ LH2). In total 37 experiments were performed, not counting shake-down tests, pre-cooling and instrumentation checks. Table 1 gives the pressure and temperature measured at the "cross" close to the release nozzle, the observed steady-state hydrogen mass flow through the nozzle, and the nozzle diameter for each test.

Table 1: ICESAFE experiments with cryogenic hydrogen release

Exp. no.	P (bar)	T (K)	Massfl. (g/s)	D_{nozzle} (mm)
3000	19	37	4.55	1
3001	7	34	3.33	1
3002	15	38	4.28	1
3003	35	65	3.31	1
3004	29	36	8.02	1
3005	18	36	6.55	1
3006	7	34	3.22	1
3007	11	36	4.01	1
3008	25	45	3.08	1
4000	12.99	37.46	4.89	1
4001	11.60	38.60	4.03	1
4002	12.60	37.80	4.62	1
4003	11.98	39.10	4.35	1
4004	13.40	40.90	4.97	1
4005	26.35	42.38	8.03	1
4006	27.05	40.04	7.56	1
4007	27.01	39.89	7.76	1
4008	27.50	38.79	7.39	1
4009	27.18	38.24	7.55	1
4010	13.08	38.41	4.72	1

Exp. no.	P (bar)	T (K)	Massfl. (g/s)	D_{nozzle} (mm)
5000	29.85	43.59	2.07	0.5
5001	29.85	43.59	2.07	0.5
5002	29.85	43.59	2.07	0.5
5003	29.85	43.59	2.07	0.5
5004	29.85	43.59	2.07	0.5
5005	29.85	43.59	2.07	0.5
5006	29.85	43.59	2.07	0.5
5007	29.85	43.59	2.07	0.5
5008	29.85	43.59	2.07	0.5
5009	29.85	43.59	2.07	0.5
5010	29.85	43.59	2.07	0.5
5011	29.85	43.59	2.07	0.5
5012	29.85	43.59	2.07	0.5
5013	29.85	43.59	2.07	0.5
5014	29.85	43.59	2.07	0.5
5015	29.85	43.59	2.07	0.5
5016	29.85	43.59	2.07	0.5

In the series IF3000 the facility was pre-cooled by a 1 g/s hydrogen flow through the bypass before each test, where the switching of the flow from the bypass to the release nozzle caused a change in the measured reservoir conditions. The left graph of Fig. 2 shows measured reservoir pressures, temperatures and H_2 mass flow rates during the release period (0 – 13 s) for an example (IF 3004) in which at a high H_2 flow rate the pressure in the system had to be increased substantially to keep the mass flow constant. This effect was due to slight heating of the hydrogen flow in the less precooled end pipe section leading to the nozzle that was merely isolated with Armaflex foam.

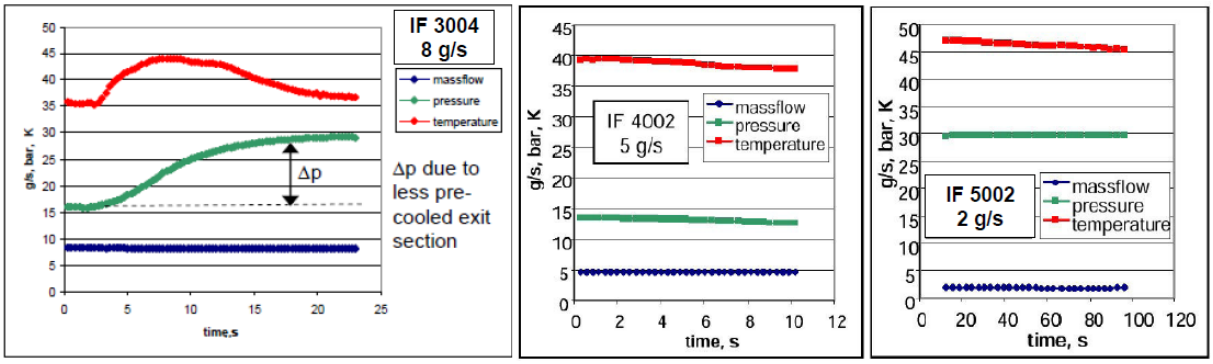

Figure 2: Examples of test conditions and measured data for the different experiment series. Pre-cooling of the exit branch for 100 s (series IF4000 and IF5000) leads to much more constant process parameters than in the IF300 series.

To achieve more constant reservoir conditions in the following two test series, the entire facility was first cooled down with a flow of about 1 g H_2/s for 1.5 hours as before with the hydrogen flow being discharged through the bypass line to the environment. However, for better pre-cooling of the exit branch the cryogenic hydrogen was then directed through the nozzle and removed by a special ventilation for about 100 s before the release of cold H_2 into the test chamber. This test procedure indeed resulted in much more constant reservoir conditions (centre and right graph in Fig. 2) compared to the IF 3000 series, which confirms that the pressure increase observed in the IF 3000 tests was related to a small temperature increase of the hydrogen in the exit branch.

In the test series IF3000 and IF4000 a 1 mm nozzle was used for distribution and combustion tests, while in the series IF5000 both kinds of tests were performed with a smaller nozzle of 0.5 mm diameter to allow scaling of the results. Fig. 3 shows typical instrumentation of the distribution and combustion tests (GM = gas sample taking cylinder, T = thermocouple, WS = heat flux sensor).

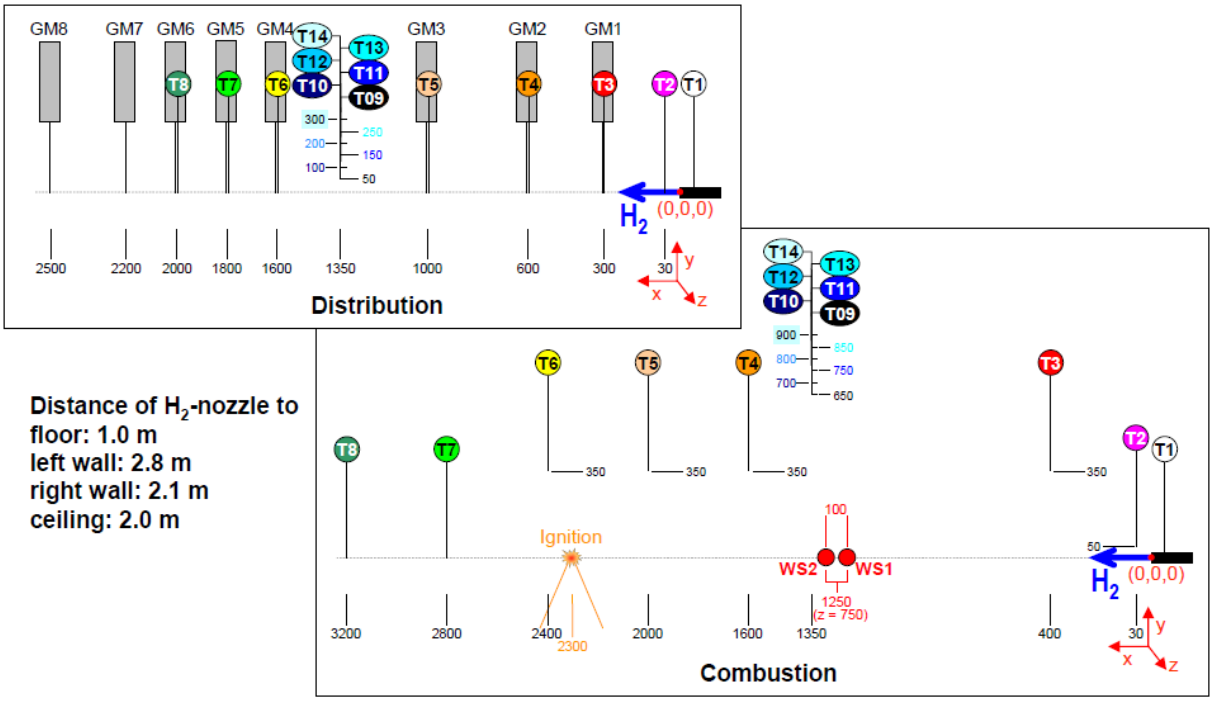

Figure 3: Typical examples for the instrumentation in the distribution and combustion experiments (GM = sample taking cylinder, T = thermocouple, WS = heat flux sensor).

Fig. 4. summarizes the reservoir conditions (measured at the cross) in a temperature-entropy plot. The shown isobars were calculated using the NIST [4] real gas equation-of-state for normal hydrogen. The figure demonstrates that all steady-state reservoir conditions obtained in the ICESAFE facility are supercritical single phase states which vary from high liquid-like to low gas-like densities (from about 50 kg/m³ in test 3004 to 6 kg/m³ in test 3001). Single phase liquid hydrogen will only exist at reservoir location if the local temperature, T, is below the critical temperature of normal hydrogen (32.2 K) and the pressure, P, is above the liquid saturation pressure at the given temperature ($P > P_{saturation}(T)$). Although the piping downstream of the LH2-bath was completely designed and built with super insulation according to state-of-the-art technology up to 10 cm before the cross, residual heat flows prevented the achievement of reservoir temperatures below 34 K.

Isentropic expansion of the reservoir state to 1 bar should lead to a two-phase flow condition with about 20 K temperature. In the present jet release experiments the situation is further complicated due to the entrainment of gaseous nitrogen and oxygen into the jet. Close to the nozzle temperatures were measured which are sufficiently low for N_2 and O_2 condensation (30 mm from the nozzle about – 200°C).

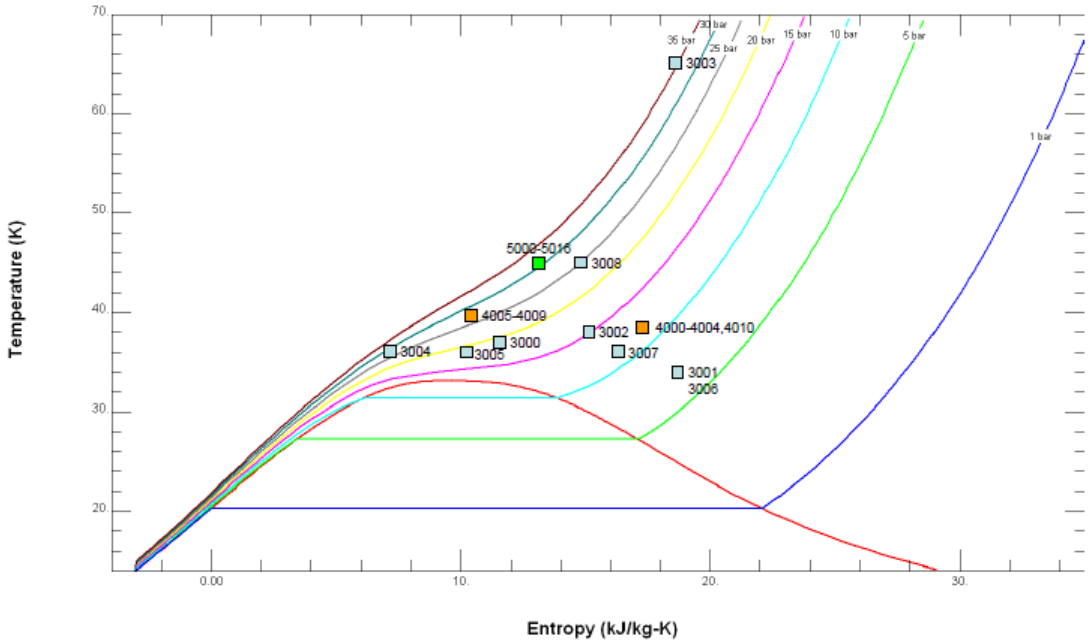

Figure 4: Measured reservoir conditions in the cryogenic release ICESAFE tests. Numbers relate to the test numbers given in Table 1.

3.1 Hydrogen concentration measurements

Hydrogen concentrations along the axis of the unignited jet were measured in the IF 3000 test series for a nozzle diameter of 1 mm and in the IF 5000 test series for a 0.5 mm – nozzle. The results of the measurements are shown in Fig. 5 as a function of the scaled distance $X = (x/d) \cdot (\rho a/\rho o)^{1/2}$.

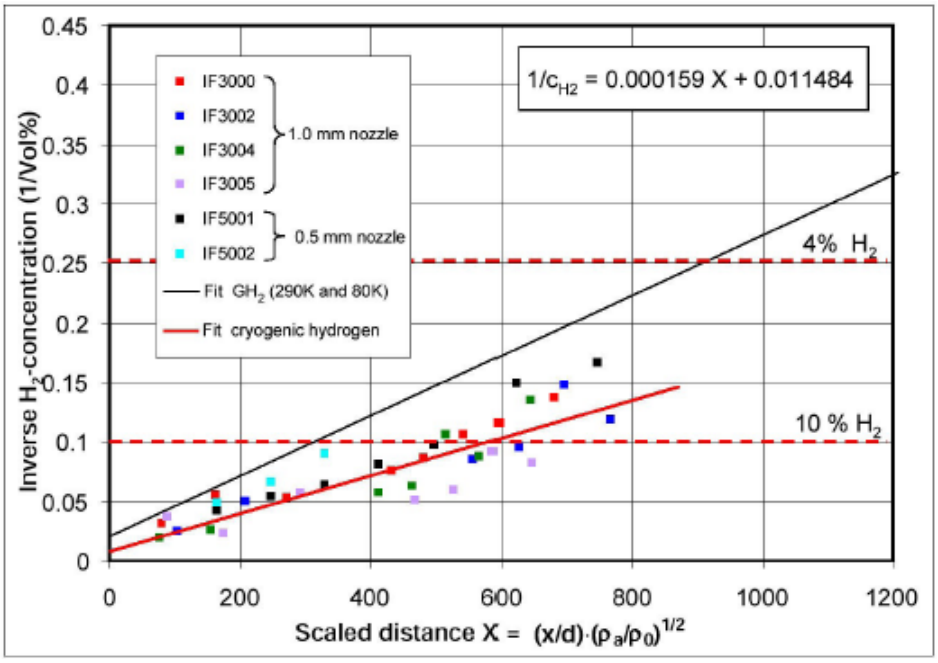

Figure 5: Summary of measured axial hydrogen concentrations in case of cryogenic H_2-release.

Although the data from a single experiment show significant scatter, the total data base of both test series indicates a uniform trend which may be represented by the least square fit:

$$1/C_{H2} = 0.011484 + 1.59 \cdot 10^{-4} \left(\frac{x}{d}\right)\left(\frac{\rho_a}{\rho_0}\right)^{1/2} \quad (1)$$

where C_{H2} – gaseous hydrogen concentration, Vol.-%, x – distance from nozzle, m, d – nozzle diameter, m, ρ_a and ρ_0 – densities of ambient air and of the cryogenic hydrogen in the reservoir. For scaled distances of X > 800 the data points show an increasing tendency to larger $1/C_{H2}$-values (smaller H_2-concentrations) due to buoyancy induced inclination of the jet trajectory, especially for small mass flow rates (exit velocities). These data points are omitted from Fig. 5 to exclude this effect and identify the undisturbed axial concentration decay in cryogenic H_2 jets (at a value of x = 1000 the data points approximately reach the line for a H_2-concentration of 4%).

Relation (1) summarizes the axial hydrogen concentrations in cryogenic jets which were measured in this project for different nozzle diameters (d) and different reservoir conditions (ρ_o). This relation is proposed to scale axial hydrogen concentrations to other values of d and ρ_o.

3.2 Scaling of hydrogen combustion regimes

Depending on the ignition location three different combustion regimes were observed for cryogenic jets in the IF5000 experiment series: I) flame flash-back and stable diffusion flame at the nozzle, II) stable distant burn without flash-back, and III) unstable transient burn with quenching. To make predictions for other leak scenarios with different leak sizes and reservoir conditions the observed scaled distances of the IF5000 experiment series for flame flash-back x_{FB} and maximum ignition distance x_{IG} are used. The limit for flash-back x_{FB} describes the border between the above combustion regimes I) and II), whereas the maximum ignition distance x_{IG} defines the border between II) and III). The measured scaled distance for flame-flash back is:

$$X_{FB} = \frac{x_{FB}}{d}\left(\frac{\rho_a}{\rho_0}\right)^{1/2} = 639 \quad (2)$$

where x_{FB} - largest distance observed for flame flash-back in the IF 5000 series (= 1500 mm), d - nozzle diameter in IF 5000 tests (= 0.5 mm), ρ_a - air density (= 1.18 kg/m^3), ρ_0 - reservoir density in IF 5000 tests (= 26.0 kg/m^3). With known X_{FB} Eq. (2) can be used to predict the absolute distance for flame flashback x_{FB} (in m) for other leak diameters d (in mm) and reservoir densities ρ_0 (in kg/m^3) in the following way:

$$x_{FB} = 0.588d \cdot (\rho_0)^{1/2} \quad (3)$$

The absolute distance for flame flash-back x_{FB} depends on d and ρ_0, where ρ_0 is a function of reservoir density and temperature. Fig. 6 presents an easy-to-use plot for evaluation of Eq. (3).

On the left- hand side of Fig. 6 the reservoir density ρ_0 can be found from reservoir temperature and pressure. Point A represents e.g. the conditions of the IF 5000 test series (29.8 bar, 43.6 K, ρ_0 = 26 kg/m^3). The right-hand side graph is a contour plot of x_{FB} (ρ_0, d). The maximum distance for flame flash-back in case of a 0.5 mm nozzle is given by Point B (= 1.5 m, as measured in IF 5000 test series). For a 4 mm leak this distance would be about 12 m, as indicated by Point C.

The scaling proposed by Eq. (3) is based on the assumption that the different combustion regimes mainly depend on the hydrogen concentration at the point of ignition, and that the axial H_2-concentration in the jet can be scaled with Eq. (1). GH2-release experiments, that were made in a much larger number than the cryogenic tests in the same facility [5], showed consistently that spontaneous flame acceleration and flame flash-back is possible only for more than 11 Vol% H_2. This fact supports the scaling assumed in Eq. (3) and Fig. 6.

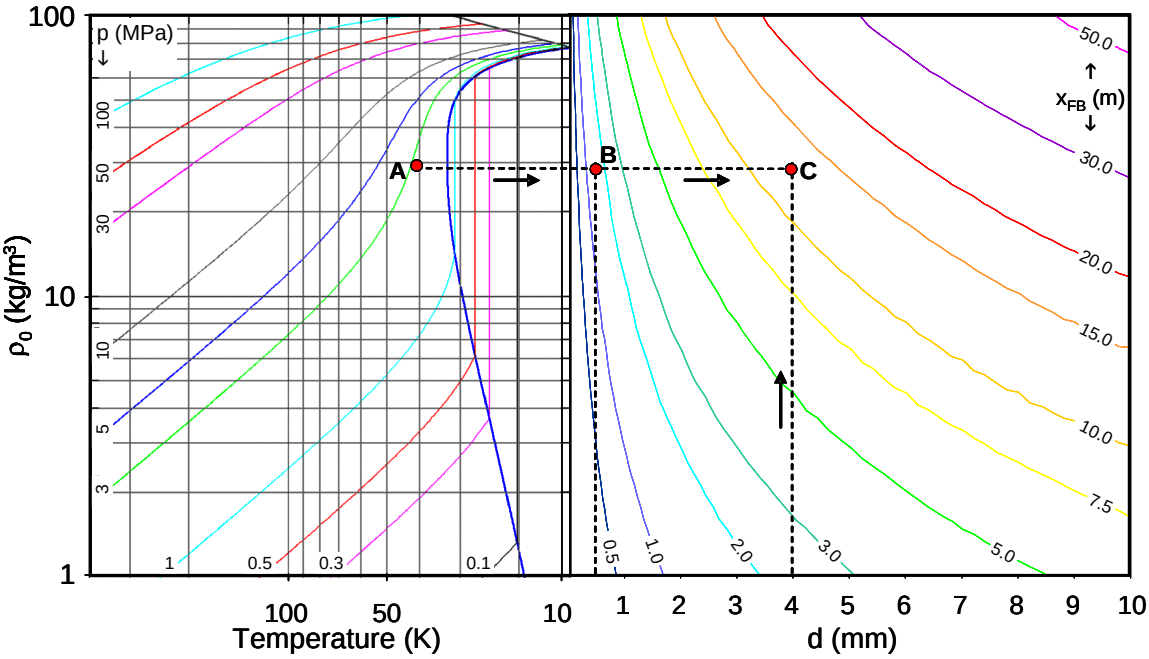

Figure 6: Prediction of maximum distance for flame flashback and stable diffusion flame for release of cryogenic hydrogen from an orifice of diameter d.

The maximum ignition distance observed in the IF 5000 experiments was x_{IG} = 1.9 m. This leads to a scaled distance of X_{IG} = 809, analogous to Eq. (2), and a predicted absolute distance of

$$x_{IG} = 0.745d \cdot (\rho_0)^{1/2} \tag{4}$$

which corresponds to Eq. (3). Fig. 7 presents the plots which allow fast graphical evaluation of the maximum ignition distance x_{IG} for given reservoir conditions and orifice diameters d. Of course precise values can be obtained from Eq. (4).

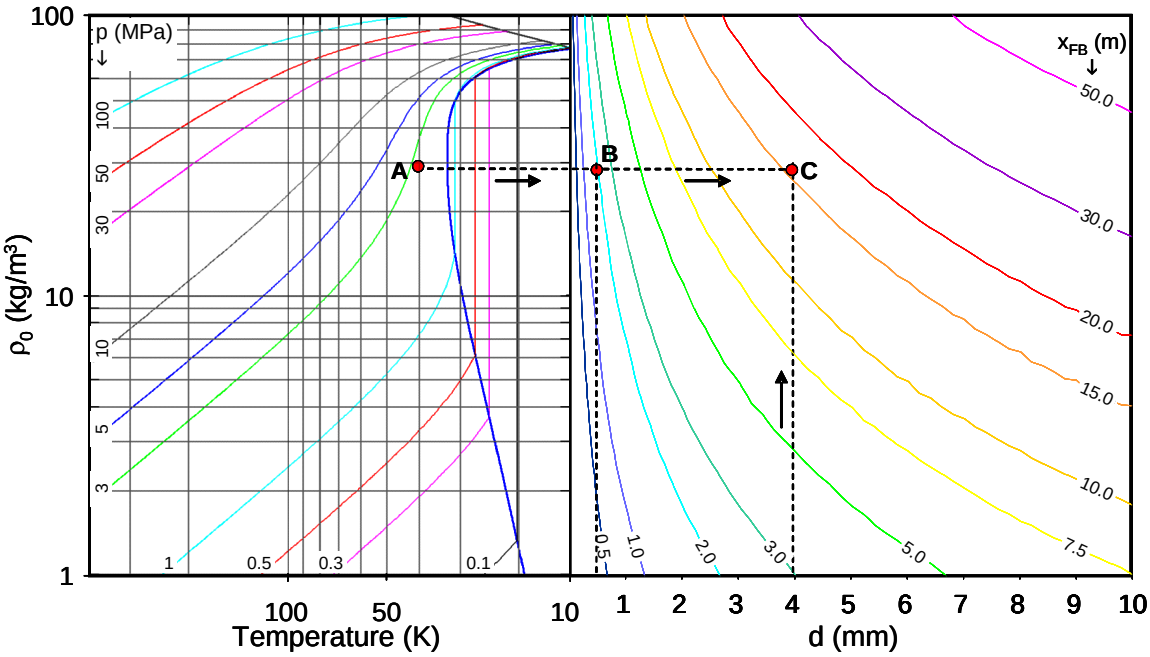

Figure 7: Prediction of maximum ignition distances for release of cryogenic hydrogen from an orifice of diameter d. Example for reservoir density of 26 kg/m^3 and orifice diameter 4 mm (x_{IG} = 15.2 m).

3.3 Thermal radiation measurements

Jet flames emit thermal radiation from the hot combustion products, which can pose a threat to persons or structures outside of the flame region. To characterize the radiation hazard from turbulent hydrogen jet flames, thermal radiation measurements were performed in the ICESAFE facility. A method for estimating total radiant output of turbulent jet flames based on the measurement of radiative heat flux at a single location is reported in [6]. In this technique the position of a wide angle heat flux sensor is varied in axial and radial direction to measure local radiation fluxes to the environment. Measurements of this type on different fuels, chemical heat release rates and burner diameters have shown that the heat fluxes can be well correlated with the visible flame length. This approach was also followed in the present study using two wide-angle sensors (150 degrees, see photographs in Fig. 8). Two different types of sensors were used to separate steam band radiation from black body radiation, if there should be important contributions. The reference point of the heat flux gauges was kept at constant temperature with a water cooling device. The axial sensor locations were 1200 and 1300 mm, respectively, and the radial distance from the jet axis was 750 mm (compare lower right part of Fig. 3).

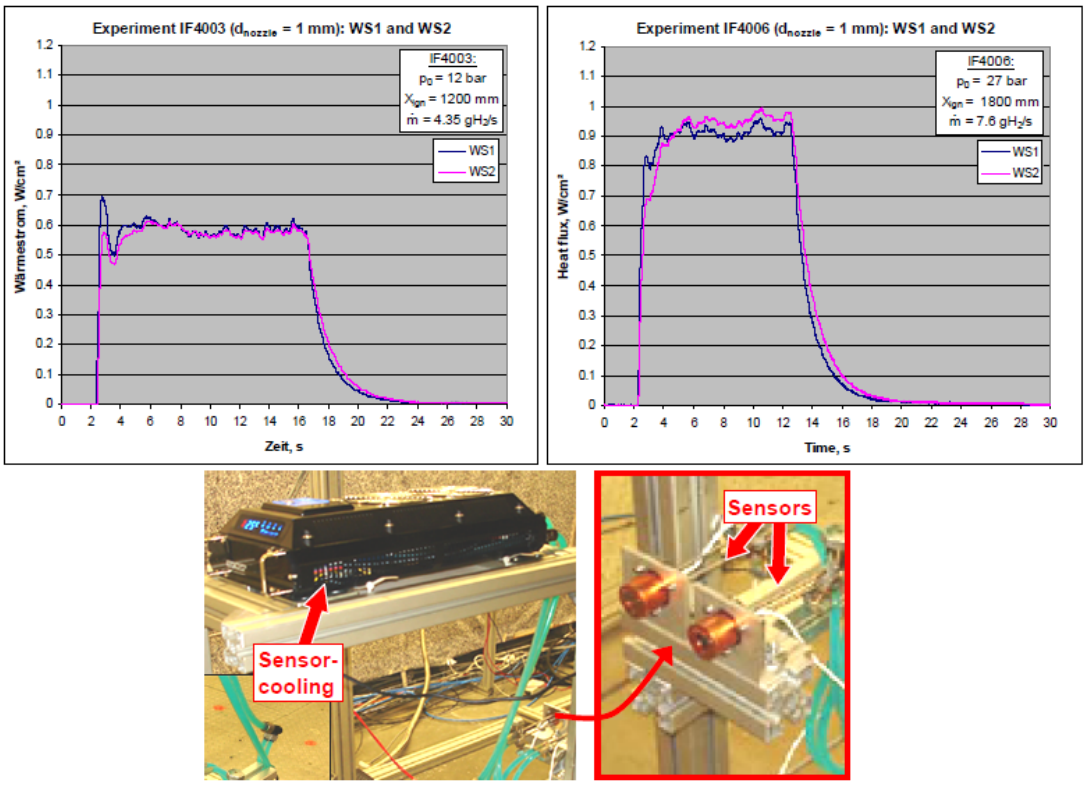

Figure 8: Two examples for measured radiation heat fluxes in the IF4000 test series (top row) and photographs of the heat flux sensors.

Two examples for measured radiation heat fluxes in the experiment series IF4000 are presented in the two graphs depicted in Fig. 8, where an experiment with the lower (12.0 bar) and one with the higher reservoir pressure (27.0 bar) are shown. In both experiments both heat flux sensors were used and a comparison of the data reveals that the two sensors agree closely in each test. The different rise times of the measured heat flux signals may be explained by the combination of two effects: I) the intrinsic time constant of the sensor, which is about 2 s as indicated by the signal decay after termination of the burn, and II) the distance between point of ignition and sensor location. In experiment IF 4003 the jet was ignited at 1200 mm, which is much closer to the position of the heat flux sensors than in IF 4006, where the jet was ignited at 1800 mm. So a clear overshoot is recorded from the first burn-out of the jet in experiment IF4003.

Furthermore it was observed that the heat flux values are correlated with the magnitude of the H_2 mass flow. As long as self-shielding of thermal radiation in the flame zone and the burned gas can be neglected, the measured heat fluxes should be proportional to the hydrogen mass flow rate of the

experiment, which is confirmed by the left graph of Fig. 9 where the measurements in an experiment of the IF5000 series, with an even lower release rate, are depicted. The other prerequisite is a sufficiently large view angle of the detectors, which appears to be fulfilled in the present experimental set-up. The right graph in Fig. 9 indicates that the heat flux measurements of all test series correlate well with each others in the form of a linear relation.

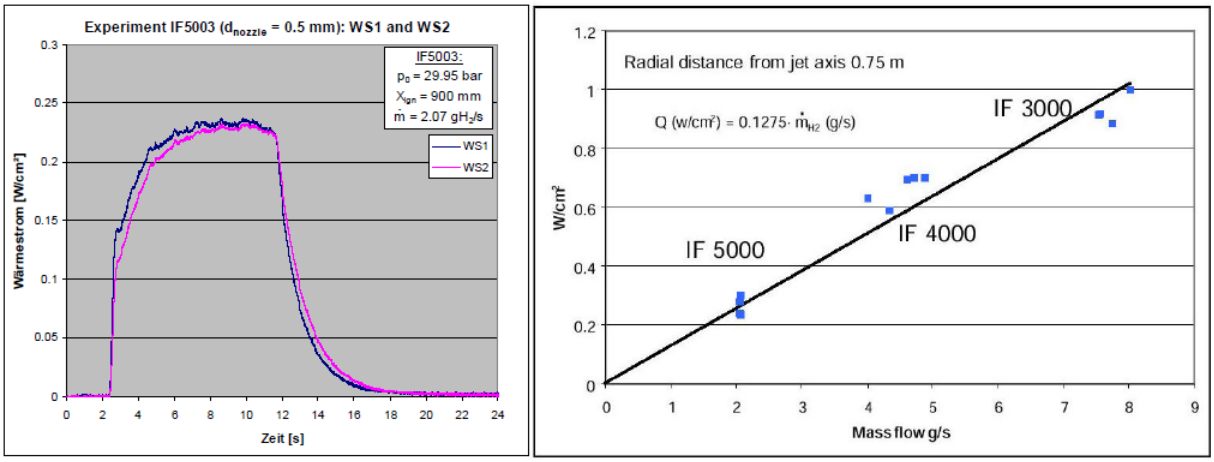

Figure 9: Radiation heat flux measurements of the IF5000 series and correlation with other test series.

The dependence of the heat flux on radial distance from the flame centre can be estimated by a point model in a first order approach:

$$Q = 4\pi r^2 q = \dot{m}\Delta H X_{rad} \tag{5}$$

With Q - total heat flux emitted, W, r - radial distance from the flame centre, m, q - measured heat flux density at r, W/cm^2, $\dot{m}$ - hydrogen release rate, g/s, ΔH - hydrogen heat of combustion, kJ/g, X_{rad} - fraction of total heat of combustion converted to radiation. This approach gives

$$q(r) = \frac{\dot{m}\Delta H X_{rad}}{4\pi r^2} \tag{6}$$

Use of the value measured for X_{rad} in the 80 K experiments, described in [5] (X_{rad} = 0.06), predicts for the heat flux q (in W/cm^2) at the sensor location:

$$q(r = 0.75m) = 0.102 \cdot \dot{m}_{H2} \tag{7}$$

($\dot{m}_{H2}$ to be introduced in g/s). This is in reasonable agreement with the experimental result given in Fig. 9. Eq. (6) may be used for first order estimates of the heat flux for other H_2 release rates $\dot{m}$ and other distances r. The relation is conservative in the sense that absorption phenomena in the flame are neglected, which may become important at much larger scales, compared to the tests performed in this project.

3.4 Sound level measurements

To investigate the potential sound level hazards from ignited cryogenic hydrogen jets, sound level measurements were performed in the test series. Four different sound level meters were installed at distances of 1.23 m, 1.65 m, 2.91 m, and 4.55 m to the release nozzle inside the test cell. In this report only the signals measured by the meter in the closest distance to the nozzle are discussed, which recorded the highest sound levels (the levels of the farther sound meters were about 2-3 dB(A) lower). The left graph of Fig. 10 displays data of the IF 3000 series, which were distribution tests without ignition. Begin and end of the stationary H2 discharge phase is characterized by noise from activating the two valves directing the hydrogen flow to the nozzle or to the bypass ("b" in Fig. 10).

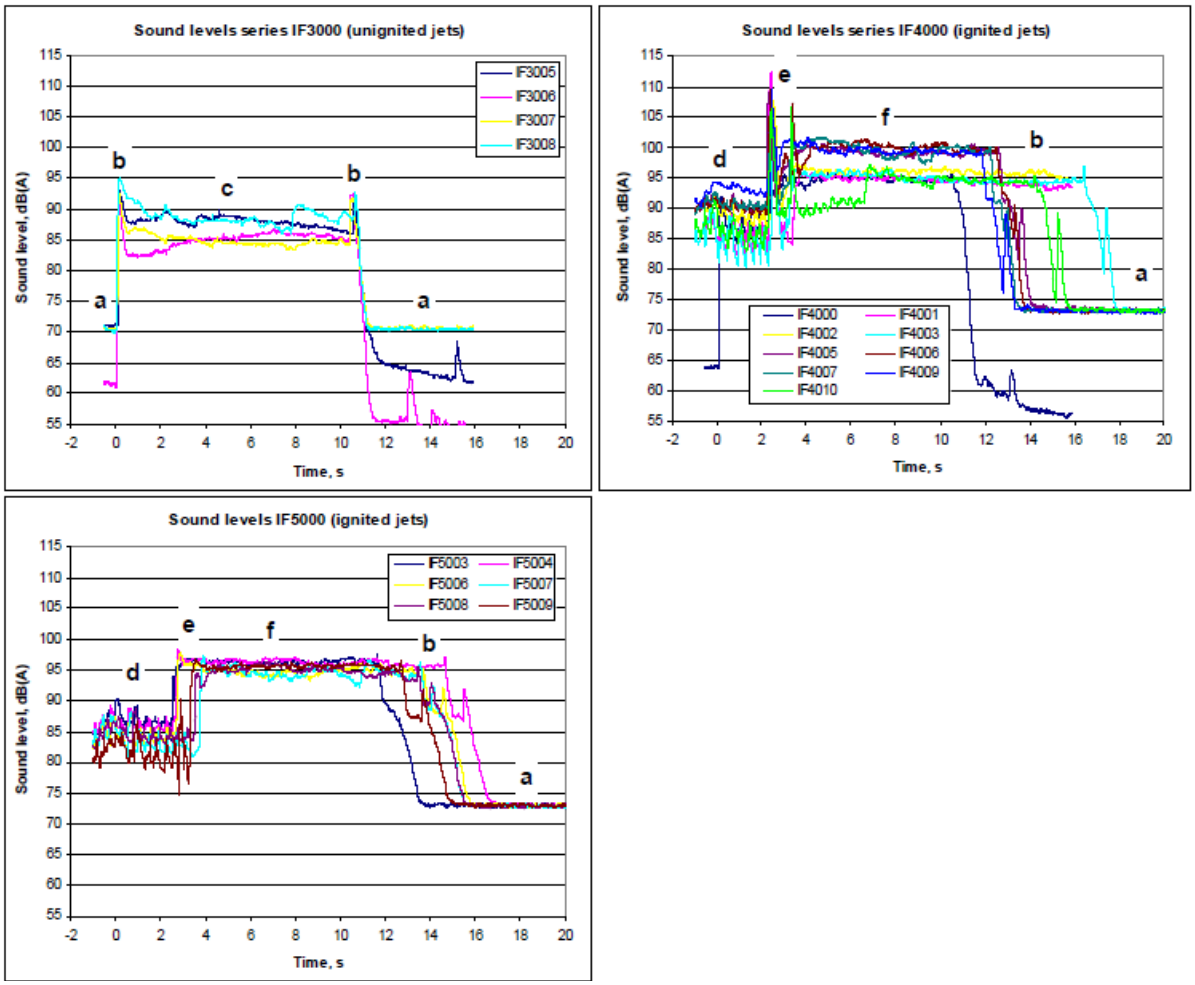

Figure 10: Sound level measurements from the different test series (a – bypass flow, b – switching of valves, c – unignited jet, d - unignited jet and camera shutter, e – ignition and first burn of H2-jet, f – stable diffusion flame anchored at release nozzle.

The centre graph of Fig. 10 shows measured sound levels from ignition and stable burn of the hydrogen jet of ignited IF4000 experiments. The sound level meter used for this diagram was located close to the photocamera and recorded the noise of the camera shutter to allow a synchronization of the pictures. The following phases of the experiments can be distinguished: unignited jet superimposed by noise from camera shutter (labelled "d" in Fig. 10), ignition and first burn-out of the H_2 cloud existing in the test chamber ("e" in Fig. 10), stationary diffusion flame anchored at the release nozzle ("f" in Fig. 10), and termination of test by valve operation ("b" in Fig. 10). The highest sound levels are measured shortly after ignition, reaching up to 112 dB (A). The reason can be clearly identified from optical pictures and BOS images taken during the ignition phase. Fig. 11 shows processed BOS-photos from experiment IF4007 shortly before and after the jet ignition. Fast burn-out of the partly premixed hydrogen inventory in the jet occurs in the third frame, and causes the highest sound emission during the whole test. In the BOS image a large cloud of expanding burned gases can be identified. The hot gas cloud then shrinks in size due to the establishment of a stable diffusion flame (last two frames in Fig. 11).

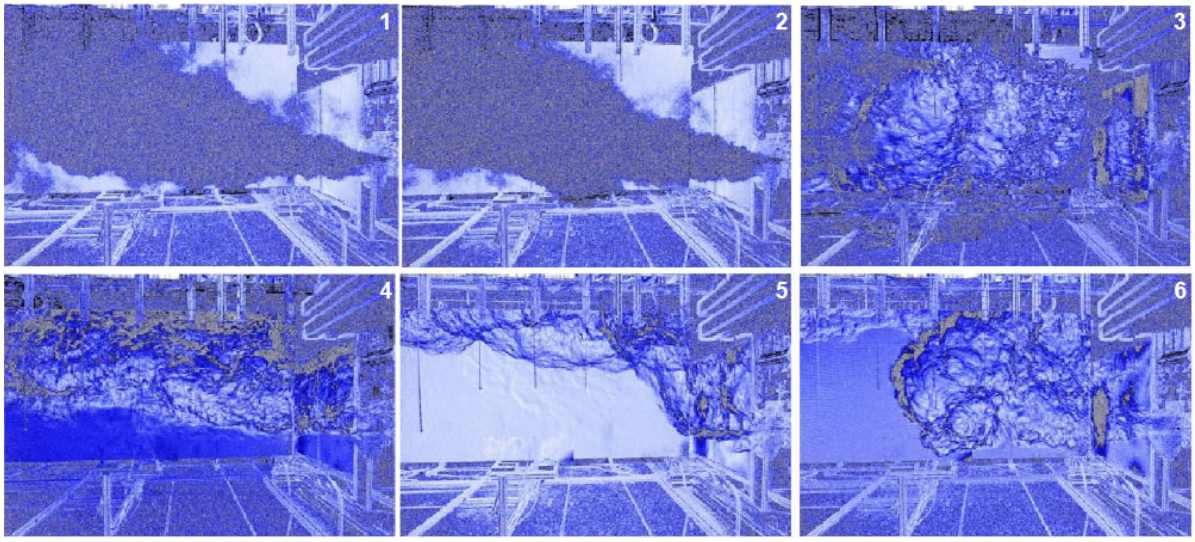

Figure 11: BOS-images of experiment IF4007 (Δt = 0.35 s). Frames 1 and 2 show the unignited cryogenic hydrogen jet. The third frame shows a large cloud of expanding burned gases shortly after ignition.

Measured sound levels from ignited IF5000 experiments are shown in the right graph of Fig. 10. The fact that in this case the ignition is not accompanied by a distinct sound signal as in the IF4000 series (centre graph of Fig. 10) is related to the smaller burnable jet volume due to the smaller nozzle diameter (0.5 mm instead of 1 mm) resulting in a much smaller cloud of burned gas after ignition.

Estimated steady-state levels of the sound meter signals are summarized in Fig. 12. Ignited jets emit about 10 dB (A) higher sound levels than unignited jets. There seems to be a weak increase of the sound level with increasing hydrogen mass flow rate. The initial burn-out of the hydrogen inventory in the unreacted jet causes the highest sound emissions.

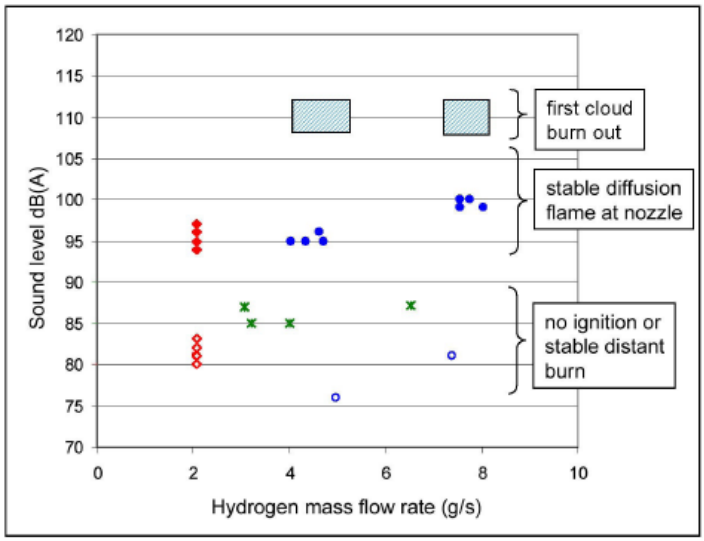

Figure 12: Measured sound levels from ignited and unignited stationary cryogenic hydrogen jets.

The sound levels summarized in Fig. 12 can be categorized with respect to their health hazard. The levels measured in this study (≤ 112 dB(A)) are considered hazardous only in case of permanent or long-time exposure. Ear damage from short sound waves becomes possible for 120 dB(A) and above [7]. So the sound emissions from unignited and ignited cryogenic hydrogen jets measured in this study pose no health hazards, even at the close distances investigated (1.2 to 4.5 m). On the other side, the measured sound levels are loud enough to allow an early identification and location of a free hydrogen jet or jet flame with sound meters.

4.0 SUMMARY

The experiments with cryogenic hydrogen releases (34 – 65 K) investigated the distribution process in unignited jets and phenomena related with the combustion in ignited jets. The hydrogen concentration measurements of experiments with different nozzle diameters and reservoir conditions (p_0, T_0) show a linear tendency when they are plotted against the density-scaled distance X (Eq. (1), Fig. 5). The measured C_{H2}-X correlation was proposed for scaling the axial hydrogen concentration to other nozzle diameters and cryogenic reservoir densities.

Three different combustion regimes were observed after the ignition of the cryogenic H2-jet: I) flash-back of the flame from the ignition source to the release nozzle under formation of a stable jet flame, II) stable distant burn close to the ignition position without flash-back, and III) transient burn with quenching of the flame. Easy-to-use diagrams were generated to estimate the maximum distance for flame flash-back x_{FB} and the maximum ignition distance x_{IG} in physical coordinates for other reservoir conditions and nozzle diameters (Figs. 6 and 7). The thermal radiation emitted by a standing cryogenic jet flame was also measured.

To investigate possible health hazards of burning cryogenic jets, overpressures and sound levels were measured during ignition and combustion. The free, unobstructed jet flames that were investigated in this study show no hazard with respect to the measured overpressures. The highest sound levels were measured shortly after the ignition and reach values of up to 112 dB(A) in a distance of a few metres of the ignition source (Fig. 12), so the maximum transient and stationary sound levels measured during this study show no hazards to exposed persons.

ACKNOWLEDGEMENTS

This work was performed within the Icefuel project (www.icefuel.de) which was co-funded by the German Federal Ministry of Education and Research. The authors are very grateful to the program manager Dr. G. Markowz for continuous support and fruitful discussions throughout this research.

REFERENCES

1. Dylla A., H_2-Transport durch Kabel. *Energieversorgung "HZwei –Das Magazin für Wasserstoff und Brennstoffzellen"*, 7. Jahrgang, April 2007.
2. Breitung W., Stern G., Veser A., Friedrich A., Kutznetsov M., Fast G., Oechsler B., Kotchourko N., Travis J.R., Xiao J., Schwall M., Rottenecker M., FINAL REPORT, Experimental and theoretical investigations of sonic hydrogen discharge and jet flames from small breaks, KIT / Research Center Karlsruhe, December 2009.
3. Klinge, F., Kirmse, T., Kompenhans, J., Application of Quantitative Background Oriented Schlieren (BOS) Proceedings of PSFVIP-4, June 3-5, 2003, Chamonix, France, paper F4097
4. Leachman J.W.; Jacobsen R.T.; Penoncello S.G., Lemmon E.W., Fundamental Equations of State for Parahydrogen, Normal Hydrogen, and Orthohydrogen, *J. Phys. Chem. Ref. Data*, **38**, 2009, pp. 721-748.
5. Veser A., Kuznetsov M., Fast G., Friedrich A., Kotchourko N., Stern G., Schwall M., Breitung W., The structure and flame propagation regimes in turbulent hydrogen jets, *Int. J. Hydrogen Energy*, **36**, 2011, pp. 2351-2359.
6. Sivathann Y.R., Gore J.P., Total radiative heat loss in jet flames from single point radiative flux measurements, *Combustion and Flame,* **94**, 1993, pp. 265-270.
7. Richmond D.R., Fletcher E.R., Yelverton J.T. and Phillips Y.Y., Physical correlates of eardrum rupture, *Ann. Otol. Rhinol. Laryngol.*, **98**, 1989, pp. 35–41.